Strange nonchaotic attractors and multistability in a two-degree-of-freedom quasiperiodically forced vibro-impact system

Gaolei Li[a], Yuan Yue[b,*], Celso Grebogi[c], Denghui Li[d], Jianhua Xie[e]

[a, b] Applied Mechanics and Structure Safety Key Laboratory of Sichuan Province, School of Mechanics and Engineering, Southwest Jiaotong University, Chengdu 610031, China

[c] Institute for Complex Systems and Mathematical Biology King's College, University of Aberdeen, Aberdeen AB24 3UE, United Kingdom

[d] School of Mathematics and Statistics, Hexi University, Zhangye 734000, China

[e] School of Mechanics and Engineering, Southwest Jiaotong University, Chengdu 610031, China

Abstract: In this work, we initially study the strange nonchaotic dynamics of a two-degree-of-freedom quasiperiodically forced vibro-impact system. It is shown that SNAs occur between two chaotic regions, but not between the quasiperiodic region and the chaotic one. Subsequently, we mainly focus on the abundant multistability in the system, especially the coexistence of SNAs and quasiperiodic attractors. Besides, the coexistence of quasiperiodic attractors of different frequencies, and the coexistence of quasiperiodic attractors and chaotic attractors are also uncovered. The basins of attraction of these coexisting attractors are obtained. The quasiperiodic attractor can transform into a chaotic attractor directly through torus break-up without passing through an SNA. The nonchaotic property of strange nonchaotic attractors (SNAs) is verified by its maximal Lyapunov exponent, and the strange property of SNAs is described by its phase sensitivity, power spectrum, fractal structure and rational approximations.

Keywords: vibro-impact system, strange nonchaotic attractors, multistability, Lyapunov exponents, basin of attraction

1. Introduction

The dynamical phenomena that we address in this work include strange nonchaotic attractors (SNAs), quasiperiodic attractors, and chaotic attractors. The quasiperiodically forced vibro-impact system has abundant dynamical behaviors. There are no results on the coexistence of SNAs and quasiperiodic attractors in vibro-impact systems [1], [2], [3]. Li et al. [1] showed that, a class of

* Corresponding author.
E-mail addresses: yueyuan2011@swjtu.edu.cn (Yuan Yue), ligaolei2018@163.com (Gaolei Li), grebogi@abdn.ac.uk (Celso Grebogi), lidenghui201111@126.com (Denghui Li), jhxie2000@126.com (Jianhua Xie),

quasiperiodically forced piecewise smooth systems have multistability. Shen et al. [3] studied coexisting SNAs in a quasiperiodically forced map and found different types of routes to coexisting SNAs. In this work, a quasiperiodically forced vibro-impact system is studied, and the strange nonchaotic dynamical behaviors of the system are studied by numerical methods. We mainly focus on the multistability in this nonsmooth system, and find three types of multistability phenomena, especially the coexistence of SNAs and quasiperiodic attractors.

Much research work has been done in theory, numerical simulations and experiments of SNAs [4], since Grebogi et al. [5] introduced the concept in 1984. An SNA has a fractal structure (like strange chaotic attractors [6], [7]), but it is nonchaotic in the dynamical sense [8]. The dynamical mechanisms of SNAs are relatively complex, but some mechanisms of SNAs are similar to chaos, such as intermittency route [9] and crisis route to chaos [10]. Heagy et al. [11] found that SNAs can be generated by the torus-doubling route in a two-frequency parametrically driven duffing oscillator. In addition, there are Heagy-Hammel route [11], fractal route [12], [13], [14], intermittency route [15], [16], [17], crisis route[18], [19], [20], and symmetry breaking route [21] that can generate SNAs.

The nonchaotic property of an SNA can be verified by numerical methods such as Lyapunov exponents and singular continuous power spectrum [11]. The methods of phase sensitivity [8], rational approximations [8], and dimensions [22] of attractors can be used to characterized the strange property of an SNA. Romeiras et al. [23] reported that SNAs have distinctive spectral characteristics, and SNAs can be distinguished from chaotic attractors and quasiperiodic attractors by specific indicators. Glendinning et al [24] showed that, for a class of quasiperiodic forced maps, SNAs exhibit sensitive dependence on initial conditions. Sathish et al. [25] showed that, if one uses two square waves in an aperiodic manner as input to a quasiperiodically driven double-well Duffing oscillator system, the response of the system can produce strange nonchaotic dynamical properties. In fact, the experimental distinction between an SNA and a chaotic attractor is still a difficult problem [26]. Gopal et al. [27] showed that the 0-1 test was helpful to detect the transition of the

system from quasiperiodic attractors to SNAs or from SNAs to chaotic attractors.

Many theoretical studies of SNAs mainly focused on skew product maps. Keller [28] studied a class of monotone incremental quasiperiodically forced map and proved the existence of SNAs. Alsedà et al. [29] generalized the results of Keller to unimodal quasiperiodically forced maps. Jäger [30] proved the existence of SNAs in quasiperiodically forced circle maps under rather general conditions that can be stated in terms of C^1-estimates. Li et al. [31] studied the quasiperiodically forced Ricker family and analyzed the existence interval of SNAs by combining theoretical and numerical methods. Ding et al. [32] showed that, for two-dimensional maps, the SNA box-counting dimension is two while the information dimension is one. Fuhrmann et al. [33] studied the properties of SNAs created in nonsmooth saddle-node bifurcations of quasiperiodically forced interval maps, determined the Hausdorff dimension, and the box-counting dimension of SNAs showed that these had distinct values.

The mechanisms of SNAs are more complex in the nonsmooth systems [1]. Paul et al. [34] studied the existence of SNAs in a model of two sinusoidal driven LCR dissipative oscillators, established different mechanisms to study SNAs. These mechanisms can be interpreted as the nonlinear interaction between quasiperiodic signals, which lead to the destruction of quasiperiodic attractors and chaotic attractors, and can be transformed into SNAs. Li et al. [35] considered a class of single-degree-of-freedom gear dynamical system with quasiperiodic forcing; SNAs are shown to exist in the nonsmooth system by numerical methods. The grazing bifurcation route was investigated by Zhang and Shen [36], which enriched the dynamical properties of SNAs. Because the existence of the grazing bifurcation, the attractor becomes a non-piecewise differentiable, turning into SNAs. Shen et al. [37] studied a piecewise logical system with quasiperiodic excitation, and pointed out that the truncation of border-collision torus-doubling bifurcation can lead to different types of SNAs.

The remaining of this paper is organized as follows. In section 2, we introduce the dynamical model which is studied in this work. In section 3, we analyse the SNAs between two chaotic intervals and determine the strange property of the attractors. In

section 4, we focus on the abundant multistability phenomena in the system. Finally in section 5 we conclude our results.

2. The mechanical model

We consider the following two-degree-of-freedom quasiperiodically forced vibro-impact system as shown pictorially in Fig. 1. The equations of motion of the system are

$$\begin{aligned} &M_1\ddot{X}_1+(C_1+C_2)\dot{X}_1-C_2\dot{X}_2+(K_1+K_2)X_1-K_2X_2+F(X_1)=P\sin(\Omega T+\tau)+Q\cos(WT),\\ &M_2\ddot{X}_2+(C_2+C_3)\dot{X}_2-C_2\dot{X}_1+(K_3+K_2)X_2-K_2X_1=P\sin(\Omega T+\tau)+Q\cos(WT), \end{aligned} \tag{1}$$

where the piecewise linear function is

$$F(X_1)=\begin{cases} K_4(X_1-B) & X_1>B,\\ 0 & -B<X_1<B,\\ K_4(X_1-B) & X_1>B. \end{cases} \tag{2}$$

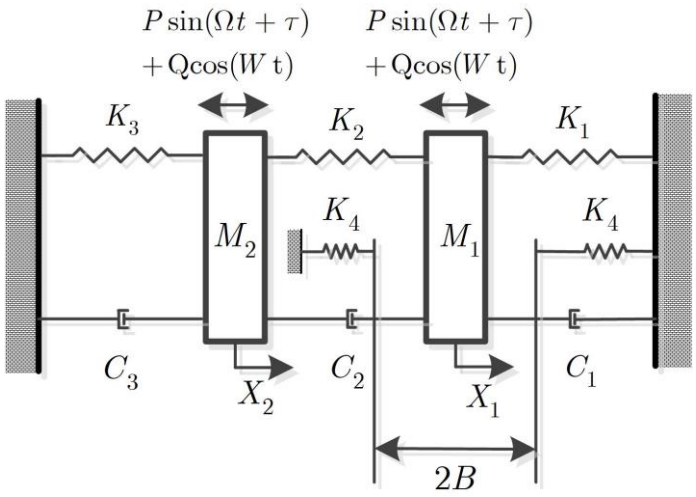

Fig. 1. The model of a two-degree-of-freedom vibro-impact system

The dimensionless form of Eqs. (1) is obtained as following. Let $\mu_m=M_1/M_2$, $\gamma_i=C_i/C_2(i=1,3)$, $k_j=K_j/K_2(j=1,3,4)$, $\omega_1=\Omega\sqrt{M_2/K_2}$, $\omega_2=W\sqrt{M_2/K_2}$, $t=T\sqrt{K_2/M_2}$, $\zeta=C_2/2\sqrt{K_2/M_2}$, $\delta=BK_2/2P$, $\varepsilon=Q/2P$ and $x_i=X_iK_2/2P$. Then Eqs. (1) can be written as

$$\begin{aligned}
&\mu_m\ddot{x}_1 + 2\zeta(\gamma_1+1)\dot{x}_1 - 2\zeta\dot{x}_2 + (k_1+1)x_1 - x_2 + f(x_1) = \frac{1}{2}\sin(\omega_1 t+\tau) + \varepsilon\cos\omega_2 t,\\
&\ddot{x}_2 + 2\zeta(\gamma_3+1)\dot{x}_2 - 2\zeta\dot{x}_1 + (k_3+1)x_2 - x_1 = \frac{1}{2}\sin(\omega_1 t+\tau) + \varepsilon\cos\omega_2 t,
\end{aligned} \tag{3}$$

where
$$f(x_1) = \begin{cases} k_4(x_1-\delta) & x_1 > \delta,\\ 0 & -\delta < x_1 < \delta,\\ k_4(x_1-\delta) & x_1 < \delta. \end{cases} \tag{4}$$

Let $\Phi = \omega_1 t$ and $\theta = \omega_2 t$, then Eqs. (3) can be transformed into the following state equations,

$$\begin{cases} \dot{x}_1 = v_1\\ \dot{v}_1 = [\frac{1}{2}\sin(\Phi+\tau) + \varepsilon\cos\theta - 2\zeta(\gamma_1+1)v_1 + 2\zeta v_2 - (k_1+1)x_1 + x_2 - f(x_1)]/\mu_m\\ \dot{x}_2 = v_2\\ \dot{v}_2 = \frac{1}{2}\sin(\Phi+\tau) + \varepsilon\cos\theta - 2\zeta(\gamma_3+1)v_2 + 2\zeta v_1 - (k_3+1)x_2 + x_1\\ \dot{\Phi} = \omega_1\\ \dot{\theta} = \omega_2 \end{cases} \tag{5}$$

According to Eqs. (3), we select ω_2 as the angle variable, which yields a three-dimensional Poincaré map

$$\begin{aligned}
&\Pi : \Sigma \to \Sigma :\\
&\Sigma \equiv \left\{(x_1, v_1, x_2, v_2, \theta) \in R\times R\times S^1 \,\middle|\, \theta \bmod 2\pi/\omega_2 = 0\right\}.
\end{aligned} \tag{6}$$

This map has the form

$$\begin{aligned}
x_{n+1}^1 &= f_1(x_n^1, v_n^1, x_n^2, v_n^2, \theta_n),\\
v_{n+1}^1 &= f_2(x_n^1, v_n^1, x_n^2, v_n^2, \theta_n),\\
x_{n+1}^2 &= f_3(x_n^1, v_n^1, x_n^2, v_n^2, \theta_n),\\
v_{n+1}^2 &= f_4(x_n^1, v_n^1, x_n^2, v_n^2, \theta_n),\\
\theta_{n+1} &= \theta_n + \frac{2\pi}{\omega_2} \pmod{2\pi/\omega_2},
\end{aligned} \tag{7}$$

where f_1, f_2, f_3 and f_4 are determined from Eqs. (5). In this work, we take $\omega_2 = (\sqrt{5}-1)/2$ as the inverse of the golden ratio. The dynamics of the system in the θ-axis is ergodic, and the trajectory starting from any initial condition can cover the

θ-axis densely. If the attractor is non-piecewise differentiable, the attractor is strange.

3. SNAs between two chaotic intervals

In general, SNAs occur between quasiperiodic and chaotic attractors in parameter space [38]. The quasiperiodic attractor can go into an SNA by different routes (such as: fractal route, torus-doubling route, intermittency route, crisis route, and others). If the parametric region of SNA existence is small, the SNAs evolve into chaotic attractors with small change of the system parameter. Here we find that SNAs are present between two chaotic intervals.

3.1 The evolution of SNAs

We consider the system parameters combination (1) $k_1=5$, $k_3=5$, $k_4=30$, τ=0, $\zeta=0.05$, $\gamma_1=2$, $\gamma_3=2$, $\mu_m=1$, and $\delta=0.02$; ε is to be taken as a control parameter. The phase diagrams on the planes (θ_n, v_n^1) and (x_n^1, v_n^1) are shown in Fig. 2, where the initial values of the system are $(x_{10}, v_{10}, x_{20}, v_{20}, \theta_0)=(0,0,0,0,0)$, and the number of iterations is 30,000, discarding the first 10,000 iterations and then plotting the next 20,000 ones. For $\varepsilon=0.052$, there is one frequency curve in the plane (θ_n, v_n^1), so there is only one invariant torus in the plane (x_n^1, v_n^1). Therefore, the system exhibits a one-torus (1T) quasiperiodic attractor, as shown in Figs. 2(a) and 2(b). For $\varepsilon=0.06$, the parameter passes through the point A (ε=0.53) in Fig. 3(d), and the system goes through torus-doubling (TD) bifurcation. There are two frequency curves in the plane (θ_n, v_n^1), so there are two invariant tori in the plane (x_n^1, v_n^1), and the system exhibits a two-tori (2T) quasiperiodic attractor, as shown in Figs. 2(c) and 2(d). For $\varepsilon=0.061$, the attractor is locally discontinuous and unstable, but the maximum Lyapunov exponent is less than 0, and the system still exhibits a 2T quasiperiodic attractor, as shown in Figs. 2 (e) and 2(f). When the parameter ε passes through the point B ($\varepsilon=0.062$) in Fig. 3(d), the maximum Lyapunov exponent will be greater than 0, the system enters into a chaotic state.

When the parameter $\varepsilon \in [0.061, 0.062]$, the 2T quasiperiodic attractor is directly transformed into a chaotic attractor. For $\varepsilon = 0.065$, the attractor loses smoothness completely, and the 2T quasiperiodic attractor becomes a chaotic attractor, as shown in Figs. 2(g) and 2(h). The maximum Lyapunov exponent $\lambda_{\max}$ is 0.042, as shown in Fig. 3(a). Fig. 3(d) shows that when the parameter ε passes through the point C ($\varepsilon = 0.079$), the maximum Lyapunov exponent is less than 0. When the parameter $\varepsilon \in [0.079, 0.0822]$, the system exhibits SNAs, as shown in Figs. 2(i) and 2(j). The maximum Lyapunov exponent in this interval is less than 0, as shown in Fig. 3(d). For $\varepsilon = 0.081$, the maximum Lyapunov exponent $\lambda_{\max}$ is -0.011, as shown in Fig. 3(b). After the Lyapunov exponent fluctuates about zero for some time, it eventually converges to a negative value, which guarantees the nonchaotic property of the attractor. The strange property of the attractor is also verified in Section 3.2, so the attractor is SNAs. When the parameter ε passes through the point D ($\varepsilon = 0.0822$), the system exhibits chaotic dynamics again. Taking $\varepsilon = 0.09$, the attractor is chaotic, and maximum Lyapunov exponent $\lambda_{\max}$ is 0.02, as shown in Figs. 2(k), 2(l) and 3(c).

In conclusion, the evolution of the attractor is as follows: 1T quasiperiodic attractor $\rightarrow$ 2T quasiperiodic attractor $\rightarrow$ chaotic attractor $\rightarrow$ SNA $\rightarrow$ chaotic attractor. Here the SNA appears between two chaotic regions, but not between the quasiperiodic region and the chaotic region.

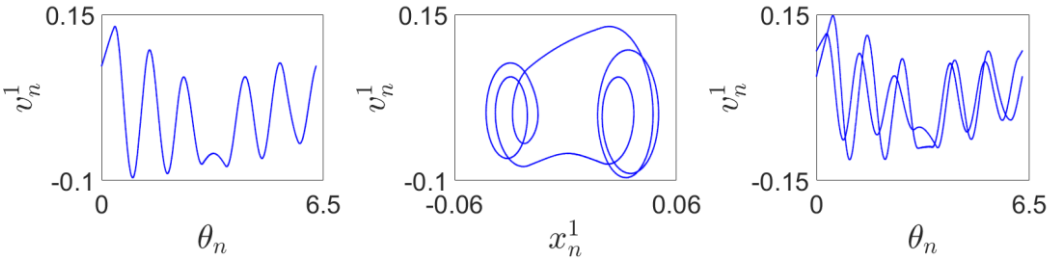

(a) (b) (c)

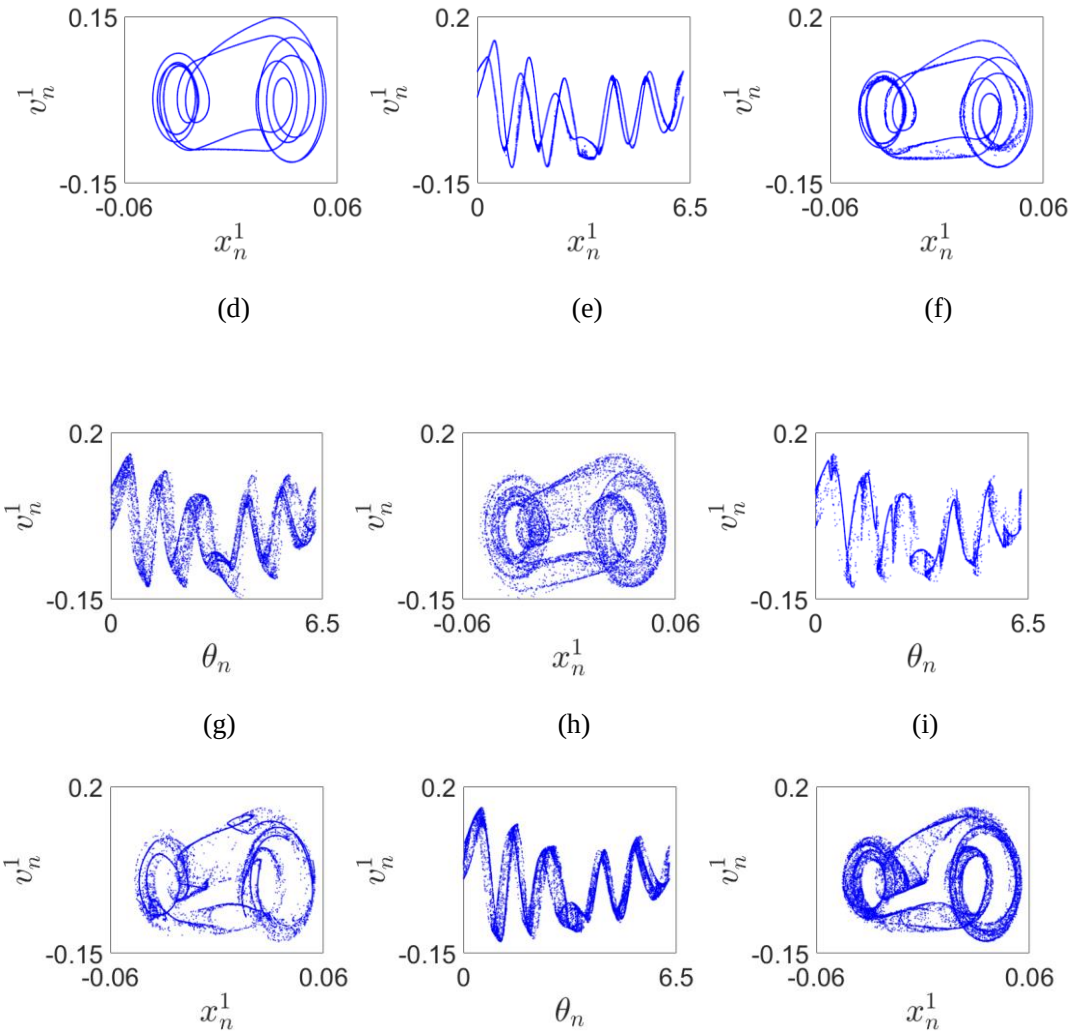

Fig. 2. The phase diagrams in (θ_n, v_n^1) and (x_n^1, v_n^1) : (a), (b) $\varepsilon = 0.052$; (c), (d) $\varepsilon = 0.06$; (e), (f) $\varepsilon = 0.061$; (g), (h) $\varepsilon = 0.065$; (i), (j) $\varepsilon = 0.081$; (k), (l) $\varepsilon = 0.09$.

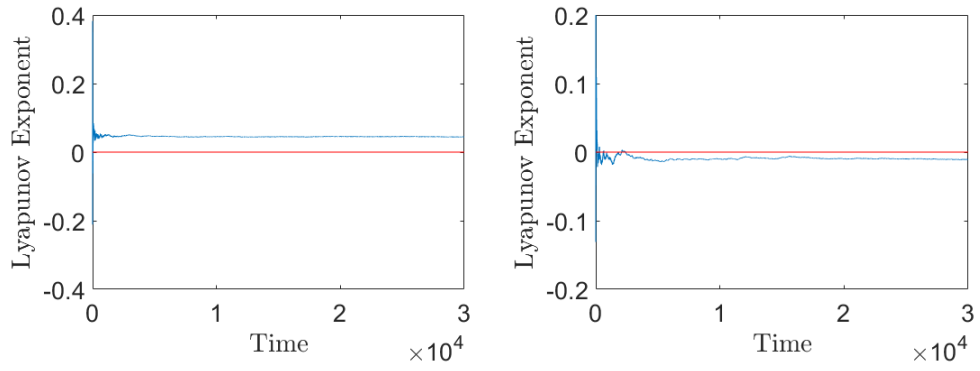

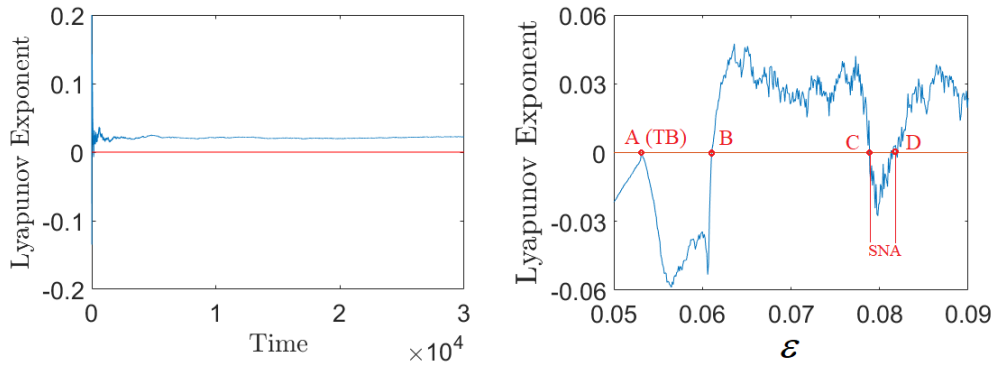

(c) (d)

Fig. 3. The maximum Lyapunov exponent: (a) $\varepsilon = 0.065$; (b) $\varepsilon = 0.081$; (c) $\varepsilon = 0.09$; (d) the maximum Lyapunov exponent with ε varying.

3.2 Determining the strange property of attractors

3.2.1 Phase sensitivity

According to the definition of SNA, SNA has the strange property which can be characterized by the phase sensitivity; the concept is based on SNA's sensitive dependence to the initial phase [8]. Because SNA is non-piecewise differentiable, there are some special bifurcation points, where the derivative value of these bifurcation points with respect to the phase is infinite. According to this property, the phase sensitivity can be used to explain that the attractor is nonsmooth. The derivative of the attractor with respect to phase can be expressed as

$$S_i^N = \frac{\partial f_i}{\partial \theta} \quad (i = 1, 2, 3, 4), \tag{8}$$

where N is the number of iterations. If S_i^N tends to a bounded value for $N \to +\infty$, the attractor is not strange. If S_i^N tends to be infinite value as $N \to +\infty$, the attractor is nonsmooth, meaning that the attracter is strange.

For a small σ, we calculate n_0 satisfying the phase difference $\varepsilon_0 = |\theta_{n_0} - \theta_0| < \sigma$, and the derivative of the dynamics with respect to phase can be approximately expressed as [35]

$$S_i^N = \frac{\partial f_i}{\partial \theta} \approx \sum_{k=1}^{N-n_0} \frac{|f_i(k+n_0) - f_i(k)|}{|\theta(k+n_0) - \theta(k)|} \ (i = 1, 2, 3, 4), \tag{9}$$

where $k+n_0 \le N$, and $f_i(n)$ denotes the nth iteration of f_i. The maximum value of S_i^N after N iterations, is denoted by

$$\tau_i^N = \max\left\{S_i^N\right\}. \tag{10}$$

If the number of iterations increases, the value of τ_i^N also increases. Then, S_i^N tends to infinite as $N \to +\infty$, and the attractor has infinite derivative with respect to the external phase, which indicates that the attractor is strange.

Let $n_0 = 4182$, then $\left|\theta(k+n_0)-\theta(k)\right| \equiv 0.000672$. Here we take SNAs in Figs. 2(i) and 2(j) as an example. For ε=0.081, the attractor is an SNA. As the number of iterations increases, the value of τ_1^N tends to infinity. For ε=0.06, the attractor is a 2T quasiperiodic attractor. As the number of iterations increases, in this case the value of τ_1^N tends to a bounded value, as shown in Fig. 4. The derivate of the attractor with respect to phase tends to infinite, indicating the non-differentiability of the attractor.

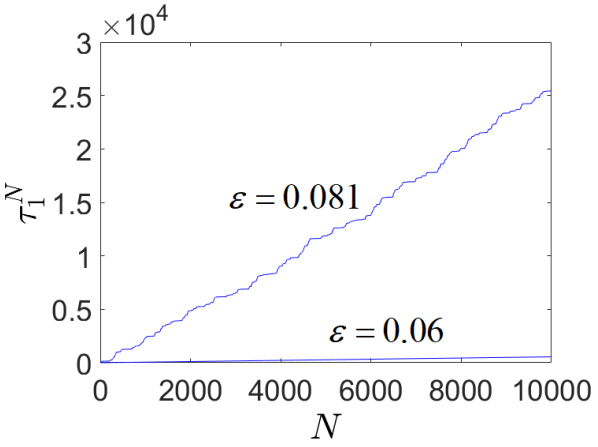

Fig. 4. The phase sensitivity of attractors.

3.2.2 Singular continuous power spectrum

Continuous and discrete power spectra are present in the dynamical systems [39]. When the system is periodic or quasiperiodic, the corresponding power spectrum is discrete, which is represented by δ-peaks at certain frequencies. For a system that undergoes chaotic or random motions, the power spectrum is continuous. However, when the system exhibits strange nonchaotic dynamics, the spectrum is a singular continuous. The power spectrum is defined as

$$P = \lim_{N\to\infty} \left| X(\omega, N)/N \right|^2, \tag{11}$$

where

$$\mathrm{X}(\omega, N) = \sum_{n=1}^{N} x_n e^{i2\pi n\omega}. \tag{12}$$

Singular continuous power spectrum is a mixture of continuous and discontinuous spectrum, which reflects the extent of the regularity of the attractor. Because SNAs exhibit a dynamical characteristic between regularity and irregularity, this special power spectrum is very important for characterizing SNAs. We take SNAs in Figs. 2(i) and 2(j), as an example. We compute the discrete Fourier transform $X(\omega, N)$ and the power spectrum P, as shown in Fig. 5. The power spectrum is continuous with many-peaks, indicating that the attractor has strange nonchaotic properties with singular continuous power spectrum.

If the attractor is periodic or quasiperiodic, then $\left|X(\omega, N)\right|^2 \sim N^2$, and for a chaotic attractor, $\left|X(\omega, N)\right|^2 \sim N^1$. If the attractor is SNAs, then it has the relation [40], [41]

$$\left|X(\omega, N)\right|^2 \sim N^{\beta}, \tag{13}$$

where $1<\beta<2$. Taking SNAs in Figs. 2(i) and 2(j), as examples, we obtain that $\beta \approx 1.78$, as shown in Fig. 6(a). Furthermore, the fractal structure of the trajectories in complex (ReX, ImX) plane are demonstrated, as shown in Fig. 6(b). Normally, SNAs occurs in the transition region from quasiperiodic attractor to chaotic one, and the exponent β is still in the transition region in terms of spectrum analysis.

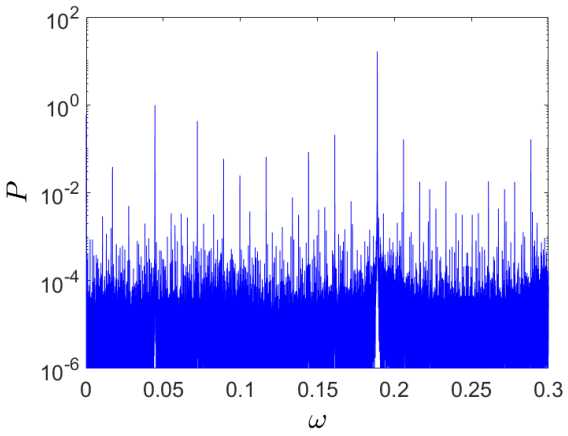

Fig. 5. For $\varepsilon = 0.081$, the power spectrum.

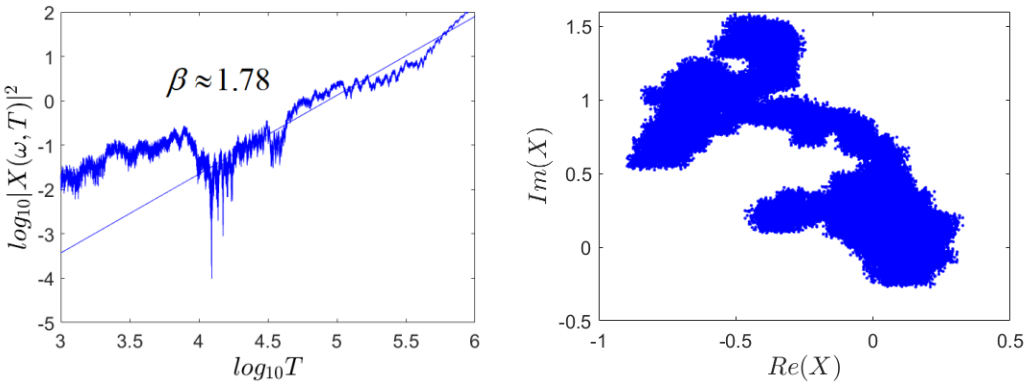

(a) (b)

Fig. 6. For $\varepsilon = 0.081$, (a) the singular continuous spectrum; (b) the fractal structure of trajectories in the complex (ReX, ImX) plane.

3.2.3 Rational approximations

Many researches show that rational approximation [8] is also a reliable method to explain the strange property of SNAs [1]. Taking $\omega_2 = (\sqrt{5}-1)/2$, the ratios of Fibonacci numbers $(w_k = F_{k+1}/F_k$, $F_{k+1} = F_k + F_{k-1}$, $F_1 = 1$, $F_2 = 1)$ are the approximants. Figure 7 shows the structure of the approximation set of an SNA at $\varepsilon = 0.081$. For different rational approximants 89/144, 610/987, 4181/6765, and 10946/17711, the phase diagrams of Poincaré map in the plane (x_n^1, v_n^1) are shown in Figs. 7(a), (b), (c) and (d), respectively. For $w_{10} = 89/144$, the order of attractor approximation is relatively low, and the shape of SNAs are not yet well-defined. Moreover, the number of such attractors is countable; the system exhibits periodic

attractor, as shown in Fig. 7 (a). For $w_{16}=610/987$, as the number of period points in the phase plane increases greatly, attractors already exhibit the shape of SNAs, as shown in Fig. 7 (b). For $w_{19}=4181/6765$ and $w_{20}=10946/17711$, the approximate attractors shown in Figs. 7 (c) and 7(d) well approximate Fig. 2 (j). As the order of approximation increases, the number of periodic points also increases, tending to the geometric fractal structure of the SNA. When the order $k\to+\infty$, it approximates the strange nonchaotic property of the quasiperiodically forced system, and the number of phase plane points tends to infinity; the structure of attractors is non-piecewise differentiable, which is described by the describe the strange property of attractors.

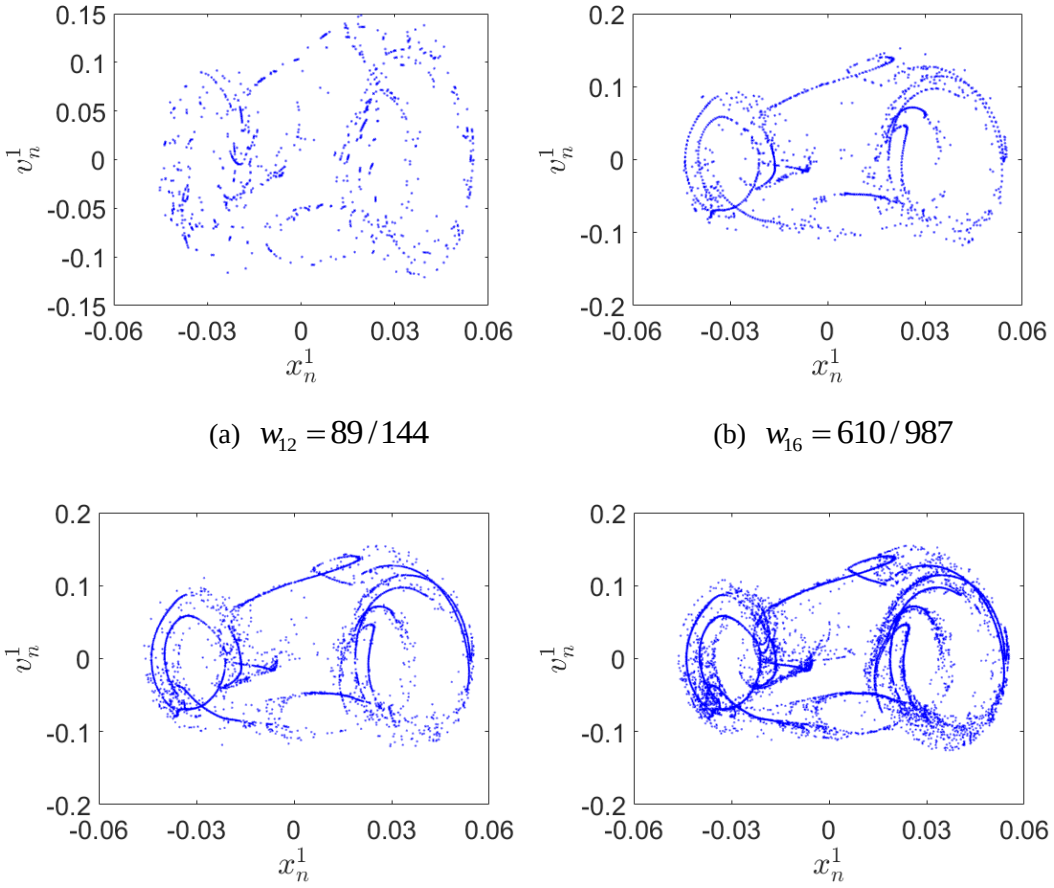

(a) $w_{12}=89/144$ (b) $w_{16}=610/987$

(b) $w_{19}=4181/6765$ (d) $w_{21}=10946/17711$

Fig. 7. Rational approximation of the SNA for $\varepsilon=0.081$ in the plane (x_n^1,v_n^1).

4. Multistability dynamics

We take the system parameters combination (2) $k_1=5$, $k_3=5$, $k_4=30$, τ=0, $\zeta=0.02$, $\gamma_1=2$, $\gamma_3=2$, $\mu_m=1$, $\delta=0.02$, and the parameter ε as the control parameter. In Fig. 8, the initial value of the blue attractor is $(x_{10}, v_{10}, x_{20}, v_{20}, \theta_0)=(0,0,0,0,0)$, and the initial value of the red attractor is $(x_{10}, v_{10}, x_{20}, v_{20}, \theta_0)=(-0.1,-0.1,0,0,0)$. For $\varepsilon\in[0.029, 0.034]$, the system exhibits the multistability phenomena [42], as shown in Fig. 8. For ε=0.025, the system has a 1T quasiperiodic attractor, as shown in Fig. 8(a). For ε=0.031, the coexistence of 1T quasiperiodic attractor (red orbit) and 2T quasiperiodic attractor (blue orbit) is shown in Fig. 8(b). For ε=0.0325, 2T quasiperiodic attractor becomes a 3T quasiperiodic attractor, and the coexistence of 1T quasiperiodic attractor and 3T quasiperiodic attractor is shown in Fig. 8(c). When ε is increased to 0.0326, the 3T quasiperiodic attractor is transformed into an SNA through the type-I intermittency route, with the maximum Lyapunov exponent $\lambda_{\max}=-0.00923$, as shown in Fig. 9(a). In this case, SNAs generated by type-I intermittency are derived from a saddle-node bifurcation in the system. Here a 1T quasiperiodic attractor coexists with an SNA, as shown in Fig. 8 (d). If the initial value is in the green region, the orbit eventually asymptotes to the SNA (blue). If the initial value is in the blue region, the orbit finally asymptote to a 1T quasiperiodic attractor (red), as shown in Fig. 10. When parameter ε is increased to 0.033, the SNA evolves into a chaotic attractor, and there is the coexistence of 1T quasiperiodic attractor and a chaotic one, the maximum Lyapunov exponent $\lambda_{\max}=0.01261$, as shown in Fig. 9(b). For ε=0.038, the blue chaotic attractor disappears, and only a 1T quasiperiodic attractor remains, as shown in Fig. 8 (f). For ε=0.04, the system goes through torus-doubling bifurcation, and becomes a 2T quasiperiodic attractor, as shown in Fig. 8(g). For ε=0.0405, a 2T quasiperiodic attractor break-up [43], and the attractor is locally discontinuous and unstable, as shown in Fig. 8 (h). For ε=0.0408, the 2T quasiperiodic attractor loses smoothness completely, evolving into a chaotic attractor, and the maximum Lyapunov exponent

$\lambda_{\max}$ is 0.00476, as shown in Figs. 8(i) and 9(c).

Summarizing, the evolution of the multistability with this set of parameters is as follows: 1T quasiperiodic attractor $\rightarrow$ 1T quasiperiodic attractor + 2T quasiperiodic attractor $\rightarrow$ 1T quasiperiodic attractor + 3T quasiperiodic attractor $\rightarrow$ 1T quasiperiodic attractor + an SNA $\rightarrow$ 1T quasiperiodic attractor + a chaotic attractor $\rightarrow$ 1T quasiperiodic attractor $\rightarrow$ 2T quasiperiodic attractor $\rightarrow$ a chaotic attractor. Here, the system exhibits not only the coexistence of the quasiperiodic attractors of different frequencies but also that of quasiperiodic attractors and SNAs. In addition, it is found that the quasiperiodic attractor does not transition through an SNA, but becomes a chaotic attractor directly.

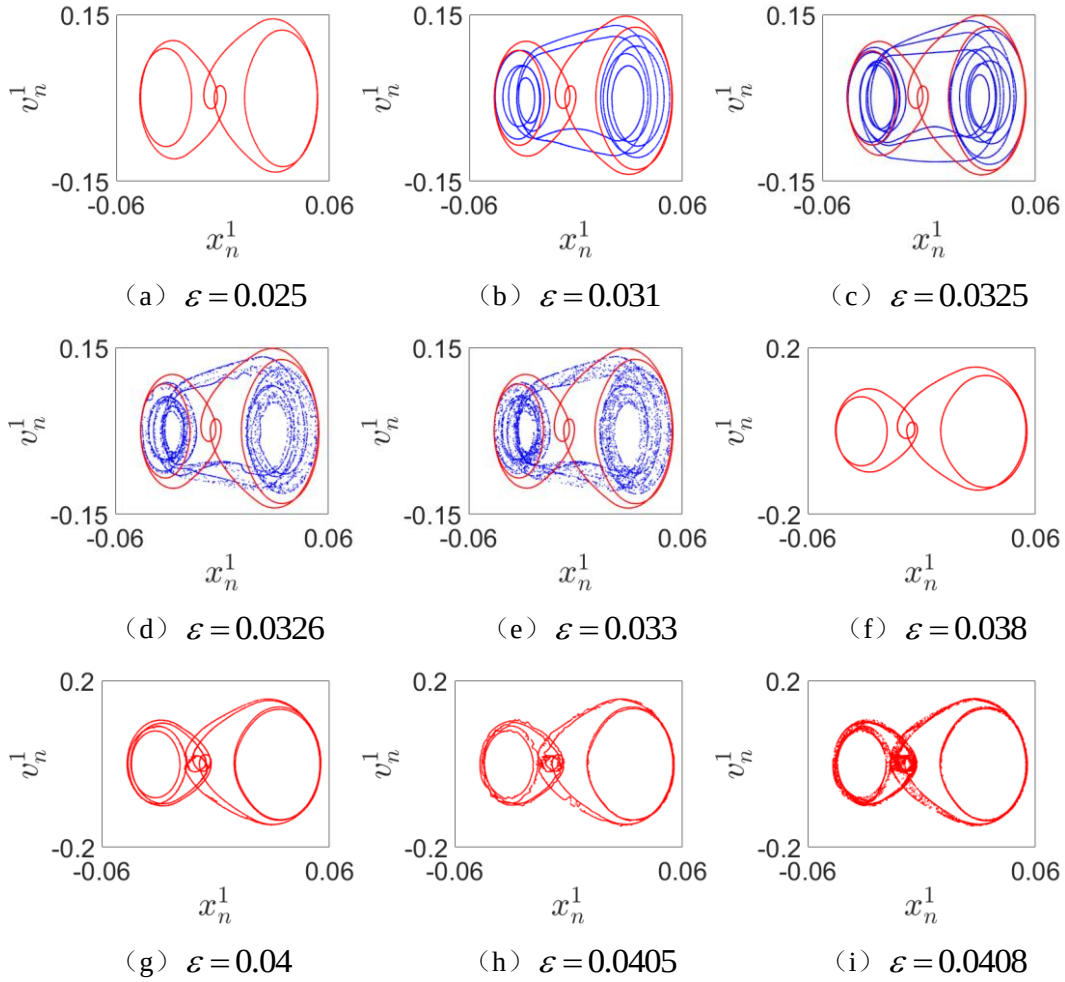

Fig. 8. The phase diagrams in (x_n^1, v_n^1).

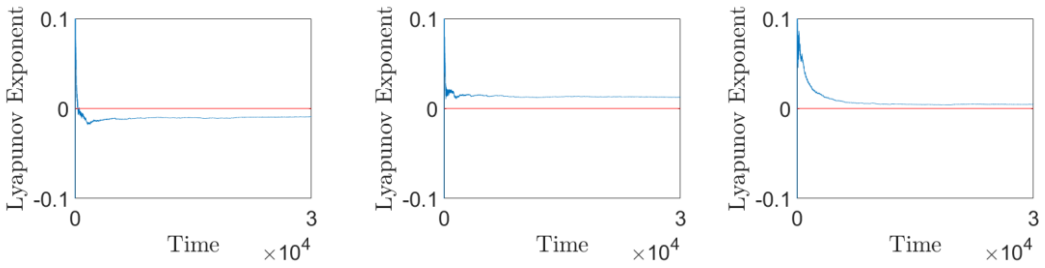

(a) ε=0.0326 (b) ε=0.033 (c) ε=0.0408

Fig. 9. The maximal Lyapunov exponent.

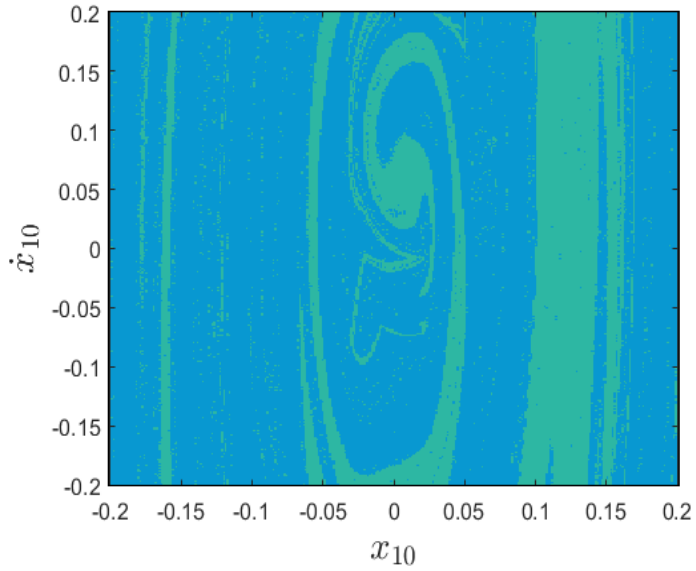

Fig. 10. For $\varepsilon = 0.0326$, the basins of attraction in the plane $(x_{10}, \dot{x}_{10})$.

Now we take the system parameters combination (3) $k_1 = 5$, $k_3 = 5$, $k_4 = 30$, τ=0, $\zeta = 0.03$, $\gamma_1 = 2$, $\gamma_3 = 2$, $\mu_m = 1$, $\delta = 0.02$, and the parameter ε as the control parameter. In Fig. 11, the initial value of the blue attractor is $(x_{10}, v_{10}, x_{20}, v_{20}, \theta_0) = (0,0,0,0,0)$, and the initial value of the red attractor is $(x_{10}, v_{10}, x_{20}, v_{20}, \theta_0) = (0.1,0.1,0,0,0)$. For $\varepsilon \in [0.0385, 0.0407]$, the system dynamics exhibits multistability. For $\varepsilon \in [0.0379, 0.0385]$, quasiperiodic attractors with different frequencies appear alternately. For $\varepsilon = 0.035$, the system exhibits 1T quasiperiodic attractor, as shown in Fig. 11 (a). For $\varepsilon = 0.0379$, another 2T quasiperiodic attractor appears, and the 1T quasiperiodic attractor (red orbit) coexists with the 2T quasiperiodic attractor (blue orbit), as shown in Fig. 11(b). For $\varepsilon = 0.038$,

the 1T quasiperiodic attractor disappears suddenly, and only the 2T quasiperiodic attractor persists, as shown in Fig. 11 (c). For $\varepsilon = 0.0381$, the 2T quasiperiodic attractor disappears suddenly, and only the 1T quasiperiodic attractor remains, as shown in Fig. 11 (d). For $\varepsilon = 0.0385$, multistability dynamics occurs again, and the 1T quasiperiodic attractor coexists with the 2T quasiperiodic attractor, as shown in Fig. 11 (e). When parameter ε is increased to 0.0405, the 1T quasiperiodic attractor evolves into a chaotic one. Here the chaotic attractor coexists with the 2T quasiperiodic attractor, and the maximal Lyapunov exponent of the chaotic attractor is $\lambda_{\max} = 0.00738$, as shown in Figs. 11(f) and 12(a). If the initial value is in the yellow region, the orbit eventually asymptotes to the 2T quasiperiodic attractor (blue orbit). If the initial value is in the blue region, the orbit eventually asymptotes to the chaotic attractor (red orbit), as shown in Fig. 13. When parameter ε is increased to 0.041, the chaotic attractor disappears, and only 2T quasiperiodic attractor exists, as shown in Fig. 11 (g). When the parameter value continues to increase to 0.042, the 2T quasiperiodic attractor breaks-up, as shown in Fig. 11 (h). For ε=0.0428, the 2T quasiperiodic attractor evolves into an SNA, which the maximal Lyapunov exponent being $\lambda_{\max} = -0.00313$, as shown in Figs. 11(i) and 12(b). For $\varepsilon = 0.045$, the SNA evolves into a chaotic attractor, whose the maximal Lyapunov exponent is $\lambda_{\max} = 0.0138$, as shown in Figs. 11(j) and 12(c).

In conclusion, the evolution of multistability dynamics is as follows: 1T quasiperiodic attractor $\rightarrow$ 1T quasiperiodic attractor + 2T quasiperiodic attractor $\rightarrow$ 2T quasiperiodic attractor $\rightarrow$ 1T quasiperiodic attractor $\rightarrow$ 1T quasiperiodic attractor + 2T quasiperiodic attractor $\rightarrow$ a chaotic attractor + 2T quasiperiodic attractor $\rightarrow$ 2T quasiperiodic attractor $\rightarrow$ an SNA $\rightarrow$ a chaotic attractor. In this example, there are not only the coexistence of quasiperiodic attractors with different frequencies, but also the coexistence of quasiperiodic attractors and chaotic attractors. Finally the quasiperiodic attractor evolves into a chaotic attractor through an SNA. It should be noted here that: (1) In the case of a single quasiperiodic attractor, another quasiperiodic attractor with different frequency can suddenly be presented, and the

coexistence of quasiperiodic attractors with different frequencies occur. (2) For the coexistence of quasiperiodic attractors of different frequencies, one of them can suddenly disappears. (3) A quasiperiodic attractor may evolve into a chaotic attractor directly without passing through an SNA.

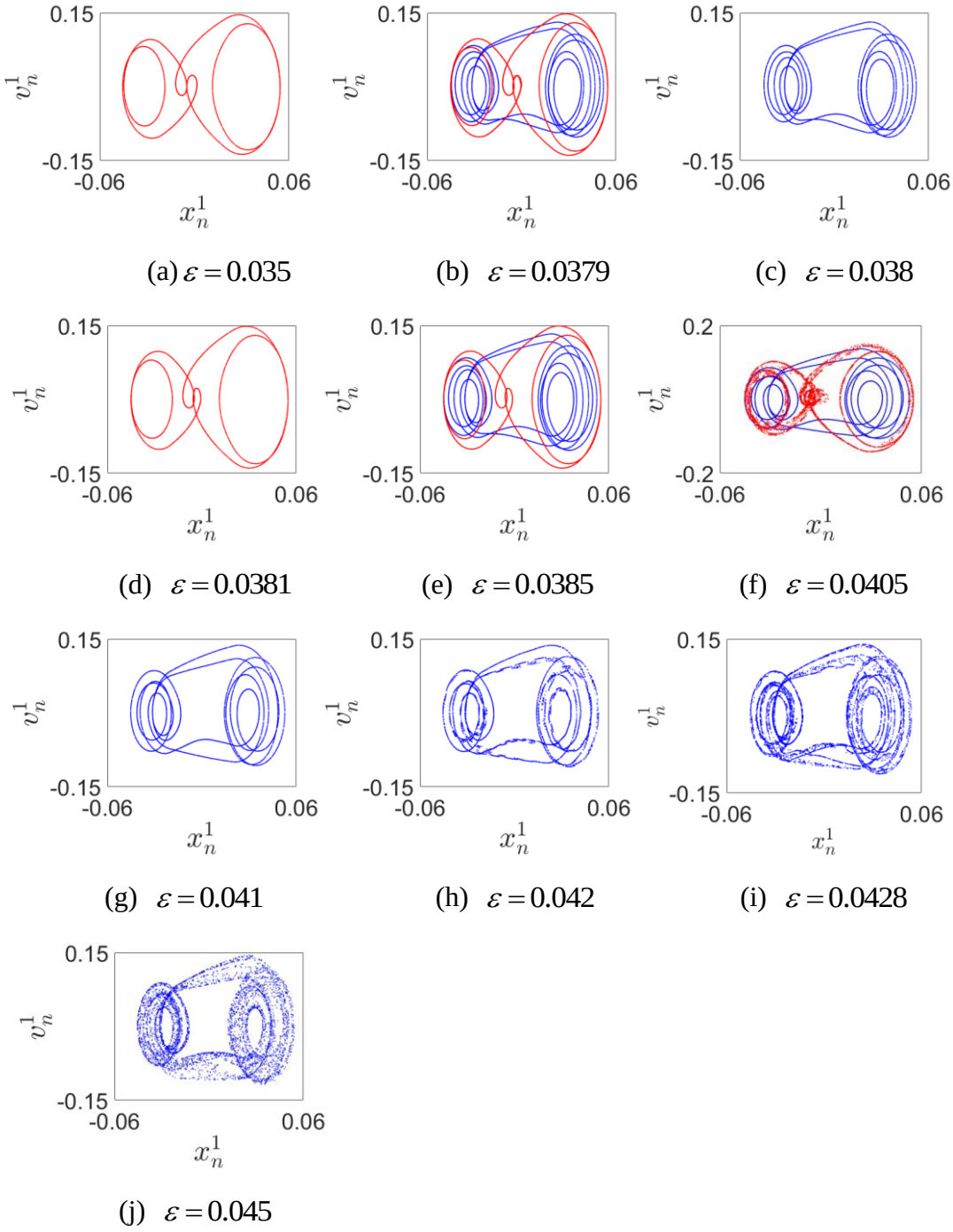

(a) $\varepsilon = 0.035$ (b) $\varepsilon = 0.0379$ (c) $\varepsilon = 0.038$

(d) $\varepsilon = 0.0381$ (e) $\varepsilon = 0.0385$ (f) $\varepsilon = 0.0405$

(g) $\varepsilon = 0.041$ (h) $\varepsilon = 0.042$ (i) $\varepsilon = 0.0428$

(j) $\varepsilon = 0.045$

Fig. 11. The phase diagrams in the plane (x_n^1, v_n^1).

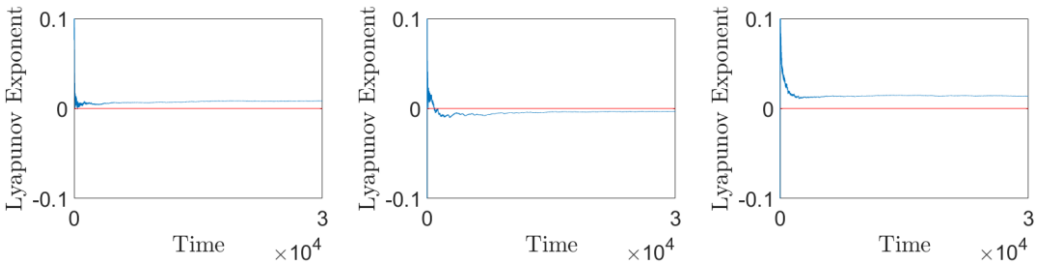

(a) $\varepsilon = 0.0405$ (b) $\varepsilon = 0.0428$ (c) $\varepsilon = 0.045$

Fig.12 The maximal Lyapunov exponent.

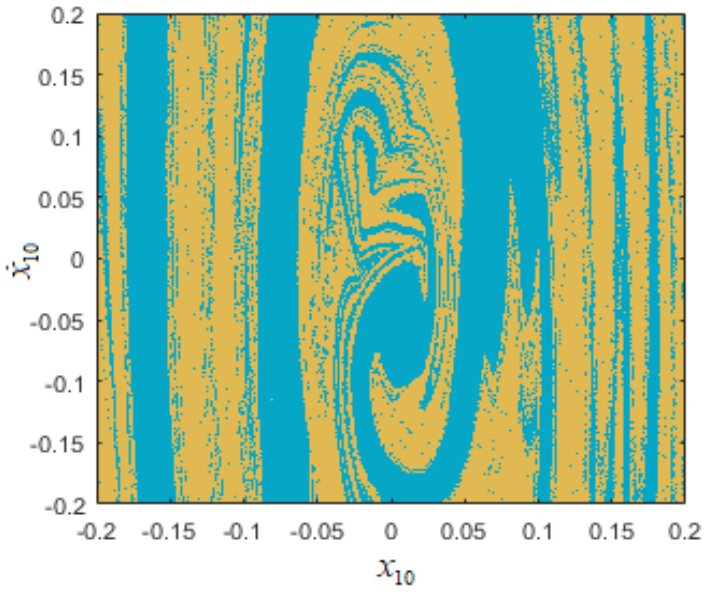

Fig. 13. For $\varepsilon = 0.0405$, the basins of attraction in the plane $(x_{10}, \dot{x}_{10})$.

5 Conclusion

In general, SNA exists between quasiperiodic attractor and chaotic attractor, but it is found in this work that SNA may exist between two chaotic regions. The nonchaotic and strange properties of an SNA are characterized by its phase diagrams, Lyapunov exponents, phase sensitivity, power spectrum, singular continuous spectrum, and rational approximations, and the basins of attraction of the coexisting attractors are obtained. It is shown that there are complex multistability phenomena in this system, including the coexistence of quasiperiodic attractors of different frequencies, the coexistence of quasiperiodic attractor and SNA, the coexistence of quasiperiodic attractor and a chaotic attractor. As the system parameter is changed, some quasiperiodic attractors do not evolve into SNAs, but directly transform into chaotic

attractors by the destruction of tori.

Acknowledgments

This work is supported by the National Natural Science Foundation of China (NNSFC) (Nos. 11672249, 12072291, and 11732014).

References

[1] G.L. Li, Y. Yue, J.H. Xie, C. Grebogi. Multistability in a quasiperiodically forced piecewise smooth dynamical system. Communications in Nonlinear Science and Numerical Simulation, 2020, 84: 105165.

[2] Y. Zhang, G. Kong, J. Yu. Critical curves and coexisting attractors in a quasiperiodically forced delayed system. Physics Letters A, 2009, 373(15): 1341-1345.

[3] Y.Z Shen, Y.X Zhang, S. Jafari. Coexistence of strange nonchaotic attractors in a quasiperiodically forced dynamical map. International Journal of Bifurcation and Chaos, 2020, 13(30): 2050183.

[4] U. Feudel, S. Kuznetsov, A. Pikovsky. Strange Nonchaotic Attractors: Dynamics between order and chaos in quasiperiodically forced systems. World Scientific, Singapore, 2006.

[5] C. Grebogi, E. Ott, S. Pelikan, J. Yorke. Strange attractors that are not chaotic. Physica D, 1984, 13(1): 261-268.

[6] Y. Li, W. Tan, K. Tan, Z. Liu and Y. Xie. Fractal and chaos analysis for dynamics of radon exhalation from uranium mill tailings. Fractals, 2016, 24(3): 1650029.

[7] F. Wen, Z. Li, C. Xie and D. Shaw. Study on the fractal and chaotic features of the Shanghai composite index. Fractals, 2012, 20(2): 133-140.

[8] A.S. Pikovsky, U. Feudel, Characterizing strange nonchaotic attractors. Chaos, 1995, 5(1): 253-260.

[9] Y. Pomeau, P. Manneville. Intermittent transition to turbulence in dissipative dynamical systems. Communications in Mathematical Physics, 1980, 74(2):189-197.

[10] C. Grebogi, E. Ott, J.A. York. Chaotic Attractors in Crisis. Physical Review Letters, 1982, 48:1507-1510.

[11] J. Heagy, W.J Ditto. Dynamics of a two-frequency parametrically driven duffing oscillator. Journal of Nonlinear Science, 1991, 1(4): 423-55.

[12]Y. Shen, Y. Zhang. Strange nonchaotic attractors in a quasiperiodically forced piecewise smooth system with Farey tree. Fractals, 2019, 27: 1950118.

[13] J.M. Kim, S.Y. Kim, B. Hunt, et al. Fractal properties of robust strange nonchaotic attractors in maps of two or more dimensions. Physical Review E, 2003, 67(3): 036211.

[14] B.R. Hunt, E. Ott. Fractal properties of robust strange nonchaotic attractors. Physical Review Letters, 2001, 87(25): 254101.

[15] A. Prasad, V. Mehra, R. Ramaswamy. Intermittency route to strange nonchaotic attractors. Physical Review Letters, 1997, 79(21): 4127-4130.

[16] A. Venkatesan, K. Murali, M. Lakshmanan. Birth of strange nonchaotic attractors through type III intermittency. Physics Letters A, 1999, 259(3-4): 246-253.

[17] S.Y. Kim, W. Lim, E. Ott. Mechanism for the Intermittent Route to Strange Nonchaotic Attractors. Physical Review E, 2003, 67(5): 056203.
[18] D. Premraj, K. Suresh, J. Palanivel, et al. Dynamic bifurcation and strange nonchaos in a two-frequency parametrically driven nonlinear oscillator. Communications in Nonlinear Science and Numerical Simulation, 2017, 50: 103-114.
[19] H.M. Osinga, U. Feudel. Boundary crisis in quasiperiodically forced systems. Physica D, 2000, 141(1-2): 54-64.
[20] A. Witt, U. Feudel, A. Pikovsky. Birth of strange nonchaotic attractors due to interior crisis. Physica D, 1997, 109(1-2): 180-190.
[21] A. Prasad, R. Ramaswamy, I.I. Satija, et al. Collision and symmetry breaking in the transition to strange nonchaotic attractors. Physical Review Letters, 1999, 83(22): 4530-4533.
[22] M. Ding, C. Grebogi, and E. Ott. Dimensions of strange nonchaotic attractors. Physics Letters. A, 1989, 137(4): 167-172.
[23] F.J. Romeiras, E. Ott. Strange nonchaotic attractors of the damped pendulum with quasiperiodic forcing. Physical Review A, 1987, 35(10): 4404-4413.
[24] P. Glendinning, T. Jäeger, and G. Keller, How chaotic are strange nonchaotic attractors, Nonlinearity 2006, 19(9), 2005-2022.
[25] A.M. Sathish, A. Venkatesan, M. Lakshmanan. Strange nonchaotic attractors for computation. Physical Review E, 2018, 97(5): 052212.
[26] S. Uenohara, T. Mitsui, Y. Hirata, et al. Experimental distinction between chaotic and strange nonchaotic attractors on the basis of consistency. Chaos, 2013, 23(2): 023110.
[27] R. Gopal, A. Venkatesan, M. Lakshmanan. Applicability of 0-1 test for strange nonchaotic attractors. Chaos, 2013, 23(2): 023123.
[28] G. Keller. A note on strange nonchaotic attractors. Fundamenta Mathematicae, 1996, 151(2): 139-148.
[29] L. Alsedà, M. Misiurewicz. Attractors for unimodal quasiperiodically forced maps. Journal of Difference Equations and Applications, 2008, 14(10-11): 1175-1196.
[30] T. Jäger. Strange non-chaotic attractors in quasiperiodically forced circle maps: Diophantine forcing. Ergodic Theory and Dynamical Systems, 2013, 33(5):1477-1501.
[31] G.L. Li, Y. Yue, D.H. Li, J.H Xie, and C. Grebogi, The existence of strange nonchaotic attractors in the quasiperiodically forced Ricker family. Chaos, 2020, 30: 053124.
[32] M. Ding, C. Grebogi, E. Ott. Dimensions of strange nonhcaotic attractors. Physics Letters A, 1989, 137: 167-172.
[33] G. Fuhrmann, M. Gröger, T. Jäger. Non-smooth saddle-node bifurcations II: Dimensions of strange attractors. Ergodic Theory and Dynamical Systems, 2018, 38: 2989-3011.
[34] A.M. Paul, K. Murali, P. Philominathan. Strange nonchaotic attractors in oscillators sharing nonlinearity. Chaos, Solitons and Fractals, 2019, 118: 83-93.
[35] G.L. Li, Y. Yue, J.H. Xie, C. Grebogi. Strange nonchaotic attractors in nonsmooth dynamical system. Communications in Nonlinear Science and Numerical Simulation, 2019, 78: 104858.
[36] Y. Zhang, Y. Shen. A new route to strange nonchaotic attractors in an interval map. International Journal of Bifurcation and Chaos, 2020, 30: 2050063.
[37] Y. Shen, Y. Zhang. Mechanisms of strange nonchaotic attractors in a nonsmooth system with border-collision bifurcations. Nonlinear Dynamics, 2019, 96: 1405-1428.
[38]M. Ding, C. Grebogi, E. Ott. Evolution of attractors in quasiperiodically forced systems: From

quasiperiodic to strange nonchaotic to chaotic. Physical Review A, 1989, 39(5): 2593-2598.
[39] Y.X Zhang, G.W Luo. Torus-doubling bifurcations and strange nonchaotic attractors in a vibro-impact system. Journal of Sound and Vibration, 2013, 332(21): 5462-5475.
[40] A.Y Jalnine, S.P Kuznetsov. Autonomous strange nonchaotic oscillations in a system of mechanical rotators. Regular and Chaotic Dynamics, 2017, 22(3): 210-225.
[41] W.L. Ditto, M.L. Spano, H.T. Savage, et al. Erratum: “Experimental observation of a strange nonchaotic attractor”. Physical Review Letters, 1990, 65(5): 533.
[42] U. Feudel, C. Grebogi. Why are chaotic attractors rare in multistable systems? Physical Review Letters, 2003, 91(13): 134102(1-4).
[43] P. Battelino, C. Grebogi, E. Ott, J.A. York. Chaotic attractors on a 3-torus, and torus break-up. Physica D, 1989, 39: 299-314.